Composites Part B 173 (2019) 106863

Contents lists available at ScienceDirect

Composites Part B

journal homepage: www.elsevier.com/locate/compositesb

Nano-featured poly (lactide-*co*-glycolide)-graphene microribbons as a promising substrate for nerve tissue engineering

Negar Abbasi Aval [a,b], Rahmatollah Emadi [a], Ali Valiani [b], Mahshid Kharaziha [a,*], Mohammad Karimipour [c,d], Reza Rahbarghazi [c,e]

[a] Biomaterials Research Group, Department of Materials Engineering, Isfahan University of Technology, Isfahan, 84156-83111, Iran
[b] Department of Anatomical Science, School of Medicine, Isfahan University of Medical Sciences, Isfahan, Iran
[c] Stem Cell research Center, Tabriz University of Medical Sciences, Tabriz, Iran
[d] Anatomical Science Department, Faculty of Medicine, Tabriz University of Medical Sciences, Tabriz, Iran
[e] Department of Applied Cell Sciences, Faculty of advanced Medical Sciences, Tabriz University of Medical Sciences, Tabriz, Iran

ARTICLE INFO

Keywords:
Polymer-matrix composites
Graphene nanosheets
Mechanical properties surface analysis
Microribbons

ABSTRACT

In this research, nanocomposite poly (lactide-*co*-glycolide)-Graphene (PLGA-Gr) microribbons were developed for neural tissue engineering. Moreover, the effects of Gr concentration (0, 0.1, 0.5 and 1 wt %) on the chemical and physical structure, mechanical properties, thermal stability and biological properties were evaluated. Our findings proved that incorporation of Gr nanosheets in the PLGA matrix resulted in the formation of aligned groove-shaped roughness on the surface of microribbons. In addition, Gr nanosheets could significantly promote the electrical conductivity and hydrophilicity of PLGA microribbons. In addition, the tensile strength and elastic modulus of the PLGA-Gr microribbons significantly promoted (upon 2 times and more than 3 times, respectively) compared to PLGA microribbons. The results demonstrated enhanced differentiation rate of SH-SY5Y cells to mature neurons on PLGA-Gr compared to PLGA. In summary, our findings discovered that aligned PLGA-Gr microribbons presented appropriate chemical, physical and mechanical properties to promote neuroblastoma cells. It is anticipated that the offered PLGA-Gr scaffolds might have great potential to develop a favorable construct for central nerve regeneration. However, further biological in vivo studies are required to assess the role of PLGA-Gr microribbons on the nerve regeneration.

1. Introduction

Central nervous system (CNS) injuries which are accompanied by nerve cell death and tissue defects could result in the permanent disability for the rest of life. Neural tissue engineering is a complex approach for clinical regeneration of damaged brain. Tissue engineering needs many factors to be involved for functional repairing of neural tissue [1]. An important factor for having successful tissue engineering process is development of a scaffold made of biocompatible and biodegradable materials for stimulating and directing the cell functions. In order to provide an ideal scaffold for neural tissue engineering, some physical properties such as porosity, surface roughness and alignment of scaffolds should be involved [2]. Moreover, in the case of neural tissue engineering, fibrous scaffolds having a high potential in the alignment of cells can end up to cell growth, migration, proliferation, and differentiation [3].

Nowadays, many researchers are working on the development of new scaffolds using a wide range of biomaterials via different techniques to establish successful constructs for regeneration of neural cells [4]. Between them, synthetic polymers like poly (lactide-*co*-glycolide) (PLGA)-based scaffolds have been investigated in neural tissue engineering thanks to their biocompatibility and biodegradability with tunable degradation rate, easy fabrication process and good mechanical strength [5]. In addition, PLGA has been widely applied as vehicles for growth factor delivery [6], cell delivery [7] and scaffolds for tissue engineering applications [8]. However, the cell affinity of PLGA is not strong enough as it is a hydrophobic polymer with lack of cell recognition site on the surface [9].

One of the pivotal factors to induce the alignment and directional growth of cells during brain development is contact guidance which is dependent on the physical shape, surface geometry and topography of the substratum [10,11]. Because of the positive effects of patterning of

* Corresponding author.
E-mail address: kharaziha@cc.iut.ac.ir (M. Kharaziha).

https://doi.org/10.1016/j.compositesb.2019.05.074
Received 28 November 2018; Received in revised form 20 April 2019; Accepted 5 May 2019
Available online 15 May 2019

the substrates on the directing the neurite growth and neural cell development, many in vitro studies have been performed on the degradable [12,13] and non-degradable substrates [14–16] with the ability to perform as a contact guidance. For instance, previous studies have demonstrated the effect of topographical features of micro-patterned PLGA on the neurite growth [16,17]. Lee et al. [18]also fabricated nanoscale ridge-groove patterns via lithography technique on a polyurethane acrylate substrate and found that this substrate was effective in directing selective differentiation of embryonic stem cells to different neural cell lines. The micro-patterned poly-methyl-methacrylate grooved surface was also reported to be helpful in mature astrocyte differentiation from radial glia-like cells without any soluble inducers [19]. One of the common and easy techniques to develop suitable contact guidance is spinning approaches such as electrospinning and wet-spinning. Wide researches revealed that aligned nano and micro-electrospun polymers could provide a contact guidance for directing neural cell growth, migration and proliferation [20–22]. In vivo studies indicated that aligned electrospun PLLA fibers could conduct neonatal nerve capillary growth along with fiber orientation to support nerve functional regeneration [23]. Another method with capability to fabricate aligned polymeric fibers is wet (solution)-spinning approach which has the ability to produce filaments with a broad range in size, shape, and morphology. Compared to the fiber morphology, formation of microribbons with higher aspect ratio could provide canal shape morphology which has more efficiency in cell attachment [24]. Besides, the small intervals between the ribbons could promote cell-cell interaction between the ribbons and as well, between different layers of ribbons. In other words, the ribbons were reported to be effective in cell sheet formation, which is potential in fabrication of functional scaffolds for tissue engineering [24,25]. Nelson et al. [26] reported the fabrication of PLGA microfilaments with repeatable wet-spinning method. They achieved PLGA microfilaments with different shapes (microfibers and microribbons) based on changing the fabrication factors. However, role of this structure on the cell behavior was not studied. Moreover, development of aligned PLGA microfilaments using wet spinning approach has not been evaluated, yet.

In order to improve the biocompatibility and surface properties of polymeric scaffolds for nerve regeneration, various researches have focused on the surface modification of the scaffolds using various types of laminin and collagen [27,28]. Since laminin and collagen are available proteins in the extracellular matrix (ECM) of neural tissue, they have been applied to surface functionalization of fibrous surface. These proteins are expensive with poor process-ability and limited availability. Therefore, other materials like polypyrrole [29], nanodiamond [30] and graphene (Gr) [31,32] have been employed for chemical and mechanical improvement of the scaffolds. Graphene and its derivatives have been widely used in biomedical applications, like biosensors, gene/drug delivery, cancer treatment and tissue engineering [33]. Gr based substrates can enhance neurite outgrowth and extension, as well as neural differentiation [34,35]. It needs to mention that, low concentration of Gr nanosheets is not cytotoxic for PC12 cells [36]. Golafshan et al. [37] applied Gr incorporated poly (vinyl alcohol)-alginate matrix using electrospinning process and reported the enhancement of PC12 cell attachment, spreading and proliferation due to increased mechanical and electrical properties of scaffolds.

Based on our knowledge, the fabrication of aligned nanocomposite PLGA-Gr microribbons using wet spinning approach has been investigated for the first time. Moreover, the role of PLGA-Gr microribbons on the neural cell function has never been investigated. The aim of this research was to provide PLGA-Gr microribbons with aligned nano-features for central nerve regeneration. In this respect, the role of various concentrations of Gr nanosheets on the various mechanical, chemical and biological properties of aligned PLGA microribbons was evaluated. It is expected that optimized PLGA-Gr microribbons might stimulate neural stem cell function.

2. Materials and methods

2.1. Materials

PLGA (50-50, $M_W = 38000–54000$ gr/mol), chloroform, dimethyl sulfoxide (DMSO) and ethanol were purchased from Sigma Aldrich. Pristine graphene nanosheets (less than 32 layers, purity> 99.5%) was purchased from Nanosany Corporation. Distilled water was used for all experiments.

2.2. Fabrication of PLGA-graphene microribbons

Aligned PLGA-Gr microribbons consisting of various amounts of Gr nanosheets (0, 0.1, 0.5 and 1 wt%) were developed using a wet-spinning method, according to the schematic presented in Fig. 1(a). After preparation of 7.5 wt% PLGA solution in chloroform at room temperature based on Nelson et al. report [26] various concentrations of Gr nanosheets were added and ultra-sonicated for 3 h to provide a uniform solution. Consequently, the solution was fed into a 3-ml plastic syringe with a blunt-ended needle with an inner diameter of 0.4 mm. The syringe was located in a syringe pump and the polymer was injected at the rate of 40 ml/min in a coagulation bath. The solution consisting of water: ethanol with a volume ratio of 2:8 was applied as the coagulation bath. In order to provide aligned microribbons, the ribbons were collected on a drum with a diameter of 100 mm. The rotation rate of the coagulation bath was considered based on the ability of fiber formation and stretching inside the bath. It was measured with a digital laser tachometer around 60 rpm. The precipitated microribbons collected on the collector had been taken out from the bath and dried in room temperature. It needs to mention that according the concentration of Gr content (0, 0.1, 0.5 and 1 wt %), the samples were named PLGA, PLGA-0.1%G, PLGA-0.5%G and PLGA-1%G, respectively.

2.3. Characterization of PLGA-graphene microribbons

The morphology of microribbons was detected using a scanning electron microscope (SEM, Philips, XL30). Before imaging, the samples were sputtered with a thin layer of gold coating. Moreover, the average diameter of microribbons was estimated on the SEM images ($n = 50$) using ImageJ software. Surface topography of microribbons was also inspected with an atomic force microscope (AFM Imaging Bruker) in tapping mode with silicone cantilevers in an air atmosphere. The water contact angle measurement was applied to estimate the hydrophilicity of the samples ($n = 3$). 5 μL water droplet was added on the surface of samples and the contact angle between the drop and the substrates was then determined via a Drop Shape Analysis System (Sessile Drop, G10). The average contact angle with standard deviation (SD) was finally reported. In addition, the four-point probe technique was applied to assess the electrical conductivity of the PLGA-Gr samples. In this regard, the samples with size of $10 \times 40\ mm^2$ were prepared and the electrical conductivity was measured.

Differential scanning calorimeter (DSC) was applied to study thermal properties of the microribbons. DSC was performed with a thermal analyzer at a heating rate of 10 °C/min under nitrogen flow with DSC 2920 TA Instruments apparatus. The chemical composition of the microribbons was also verified through Attenuated Total Reflectance-Fourier Transform Infrared spectroscopy (ATR-FTIR, Spectrum 2000). The existence of Gr nanosheets inside the microribbons was evaluated through X-ray diffraction (XRD, X'Pert Pro X-Ray diffractometer, Philips, Netherland) with CuKα radiation ($\lambda = 0.154$ nm) at a generator voltage of 40 kV and a current of 40 mA. Mechanical properties of the microribbons (with the rectangular shape with a dimension of 10 mm × 10 mm and an average thickness of 200 μm) were evaluated using a tensile tester (Hounsfiled H25KS) with a load capacity of 10 N at 5 mm/min rate. By plotting the stress-strain curves ($n = 3$), tensile strength and elastic modulus were calculated.

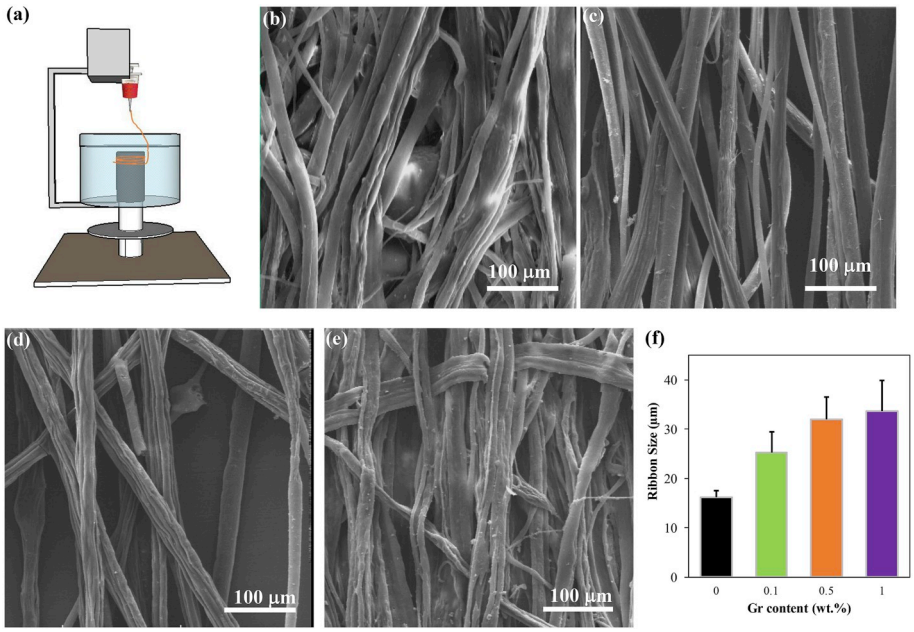

Fig. 1. Structural properties of aligned PLGA-Gr microribbons: (a) The schematic of wet-spinning process illustrating the ribbon formation injected in the coagulation bath. SEM images of (b) PLGA, (c) PLGA-0.1%G, (d) PLGA-0.5%G and (e) PLGA-1% G microribbons. (f) The average size of microribbons consisting of various amounts of Gr nanosheets (n = 20).

2.4. Cell culture

To explore the role of PLGA-Gr microribbons on the cell function, we used 3rd passage of human neuroblastoma cell line SH-SY5Y (ATCC). In this regard, PLGA-Gr microribbons (n = 3) were placed in each well of 48-well plate (SPL) and rinsed with 70% ethanol overnight. Thereafter, the wells were washed three times with phosphate buffered saline (PBS) each for 2 min. Cells were seeded at an initial density of 1.5×10^4 cells/well and incubated with Dulbecco's Modified Eagle Medium (DMEM, Sigma Aldrich) supplemented with 10% fetal bovine serum (FBS, Gibco) and 1% penicillin/streptomycin (Biosera). In order to evaluate the role of microribbons on the cell function, cell culture was performed in growth factor-free media. The plates were kept at 37 °C in a humidified atmosphere containing 5% CO_2 and were incubated over a period of 7 days.

2.4.1. Cell morphology evaluation

Cell attachment and morphological changes were studied by SEM technique. After 7 days of culture, the cells were fixed with 2.5% glutaraldehyde (Sigma) for 3 h, rinsed with PBS and dehydrated in the graded concentrations of ethanol (30, 70, 90, 100% v/v) each for 10 min. The fixed cells were air dried, gold coated and evaluated through observation by SEM.

2.4.2. Cell survival assay

At the specific time points, cell viability on the samples (n = 3) was monitored by using 3- [4, 5-dimthyl-2-thiazolyl]-2, 5-diphenyl-2-H-tetrazolium bromide (MTT) assay. For this propose, the cell seeded samples were incubated with 5 mg/ml MTT solution (Sigma-Aldrich) for 4 h. Then, the medium was discarded and each well was incubated with 400 μl DMSO for 20 min to dissolve the formazan crystals, completely. As prepared solution was pipetted into a 96-well plate to quantify the absorbance (Optical Density = OD) at 570 nm by a microplate reader (Biotek). The OD value was expressed as the percent of the control (non-treated cells).

2.4.3. Cell proliferation assay

After the completion of the incubation period, the protein level of Ki-67 was monitored via flow cytometry. It was shown that cell entering proliferation had the ability to express a nuclear factor Ki-67. Therefore, we collected cells by using enzymatic solution TrypleLE® (Invitrogen) after 7 days. Following PBS rinsing, the cells were blocked and permeabilized by using a permeabilizing buffer (eBioscience) for 20 min. Thereafter, cells were incubated with the PE-conjugated mouse anti-human Ki67 antibody (eBioscience) for 30–40 min. Then, cells were washed three times with PBS and the number of Ki-67 positive cells were calculated by the FACSCalibure system and FlowJo software version 7.6.1.

2.4.4. Cell differentiation assay

The potency of PLGA-Gr microribbons to induce differentiation toward mature neural cell type was assessed by MAP-2 after 7 days of culture. After completion of cell culture on the microribbons, cells were snap-frozen by embedding in OCT compound (Cat no: 4583; Scigen). Then, 5-μm-thick cryosections on poly-L-lysine rich slides were prepared. Slides were then exposed to 0.1% Triton X-100 (Merck) in PBS for 5 min and blocked with 3% goat serum (Invitrogen) for 30 min followed by incubation with primary antibody (MAP-2, Invitrogen, 1:500) at 4 °C overnight. After being washed with PBS for two times, the cells were incubated with Alexa Fluor 488-conjugated secondary antibody (dilution 1: 1000; Invitrogen). For counterstaining, 1 μg/ml 4′,6-diamidino-2-phenylindole (DAPI, Sigma-Aldrich) was applied to stain cell nuclei.

2.5. Statistical analysis

Data are shown in mean ± SD. In this study, at least three set of experiments were performed for each assay. To find statistical differences, we performed One-way ANOVA with Tukey post hoc analysis. $P < 0.05$ was considered statistically significant between groups.

3. Results and Discussion

3.1. Characterization of PLGA-graphene microribbons

The contact guidance of neural cells affecting by morphology of the substrate is shown to be effective on cell-cell interaction, alignment and

guidance of cells for functional recovery. Previous results revealed that, microribbons are more efficient in this application compared to fibers as they have flat cross-section and could provide edges and ridges for neural cell attachment and growth [38]. Therefore, in this study, PLGA-Gr microribbons were developed using wet-spinning process. The morphology of PLGA and PLGA-Gr constructs consisting of various amounts of Gr nanosheets (PLGA, PLGA-0.1%G, PLGA-0.5%G and PLGA-1%G) was evaluated using SEM imaging and are presented in Fig. 1(b-e). Moreover, the average diameter of the microfilaments was estimated and is presented in Fig. 1(f). SEM images confirmed the formation of microribbons in various samples, without the formation of any fiber. There are some important factors affecting the filament morphology during the wet-spinning process such as polymer concentration, coagulation solution and filaments tension [26]. According to previous researches, type of coagulation solution is a determinant parameter to control the filament morphology. For instance, it was stated that range of alcoholic type coagulants could change the cross-section of the silk filaments from circular to flat one, based on the R group size of the alcohol [39]. Therefore, based on researches performed before, we optimized the crucial parameters to get microribbons from PLGA solution (data are not show here). However, incorporation of Gr nanosheets to the polymer solution resulted in enhanced viscosity of solution. Therefore, changing the solvent and coagulant for the formation of ribbons was much more difficult than in the case of PLGA ribbon formation. Therefore, the morphology of ribbons which was based on the penetration of anti-solvent, could not be changed during the spinning [37]. In another word, with the same factors for PLGA micro-ribbon formation, we could fabricate the PLGA-Gr ones, as well, without considerable change in morphology. However, depending on the Gr nanosheet content, the size of microribbons changed. Noticeably, the size of ribbons noticeably enhanced from 16 ± 1 μm for PLGA microribbons to 33 ± 6 μm for PLGA-1%G which might be due to higher viscosity of polymer solution. Consequently, the entrance of coagulants in the PLGA-Gr microribbons would be more difficult which could hinder the formation of ribbons, leading to enhanced ribbon size. Zhang et al. [40] similarly found that with increasing the concentration of polycaprolactone (PCL) solution, the size of wet spun fibers increased.

To investigate the role of Gr nanosheets on the topography of the microribbons, AFM study was performed (Fig. 2). The results showed that the surface of PLGA microribbons was smooth without any feature. However, incorporation of 0.1 wt% Gr nanosheets (PLGA-0.1%G sample) to the microribbons resulted in the formation of minor features on the surface. Nevertheless, it seems the concentration of Gr nanosheets was not enough to make these features all along the ribbons. Increasing the concentration of Gr nanosheets up to 0.5 wt %, resulted the formation of attractive aligned and micron-sized groove-like features with average size of 0.5 μm, similar to a folded paper. The increment of Gr nanosheets to 1 wt% resulted in slightly larger grooves with average size of 1 μm, with aligned features. The formation of groove-like surface features is crucial in neural cell type attachment, alignment and successful differentiation of the cells to mature neurons [38]. Our results demonstrated that incorporation of Gr nanosheets within the PLGA solution resulted in change in the size, and surface topography of microribbons. It might be due to effective role of Gr concentration on the viscosity of the suspensions. Similarly, He et al. [37] demonstrated the effect of graphene oxide(GO) on the surface roughness of alginate-GO wet-spun fibers. They demonstrated that the roughness of the inner surface of the needle orifice in wet spinning apparatus and shrinkage of the fabricated fibers during the drying process could make an ordered striped structure on the surface which was much clearer with the addition of GO nanosheets to the polymer solution. In other words, with increasing the amount of GO in the polymer solution, they had fibers with clearly ordered striped like surface roughness. Pinto et al. [41] also demonstrated the effect of Gr and GO nanosheets on the formation of groove-shaped surface roughness with size of 1–2 μm on PLA films. Appearance of groove shaped features on the surface of the polymer-Gr and polymer-GO composite film or fibers could also be due to flexibility of Gr and Go that can rumple the polymer structure during the fabrication process [42].

In order to evaluate the role of Gr nanosheets on the hydrophilicity of PLGA, the water contact angle on surface of various samples was estimated and is presented in Fig. 3(a). Results showed that incorporation of Gr nanosheets in PLGA significantly reduced the water contact angle from $138.2 \pm 2.1^{\circ}$ to less than $116.2 \pm 1.4^{\circ}$ (after incorporation of 1 wt% Gr). It might be due to the presence of some hydrophilic OH, C–O–C and COOH groups on the Gr nanosheets. Consequently, PLGA-Gr samples could provide oxygen functional groups on their basal planes and edges leading to improved hydrophilicity of the samples. Our results

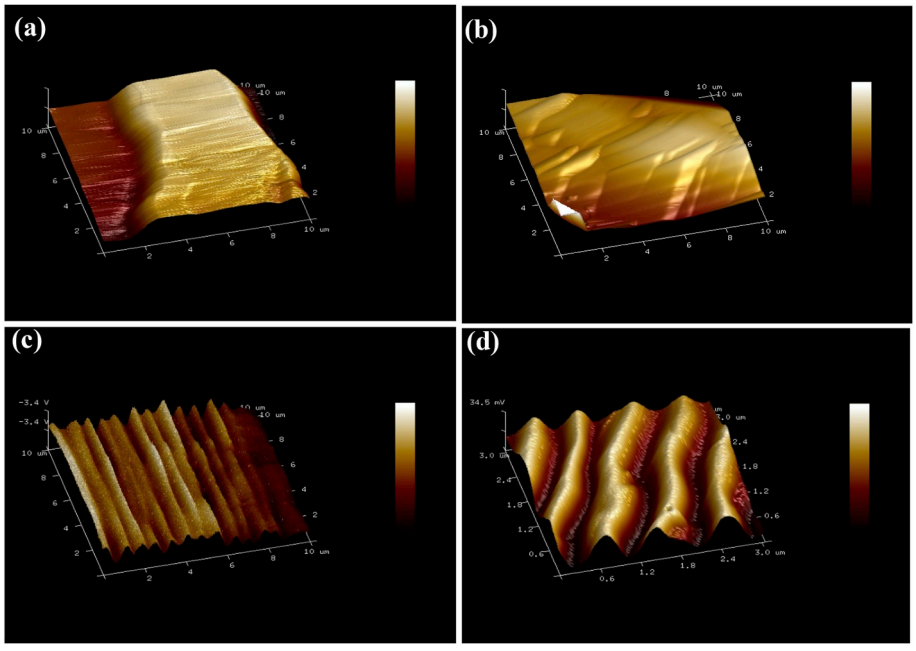

Fig. 2. Structural properties of aligned PLGA-Gr microribbons: AFM analysis for evaluating the surface roughness of (a) PLGA, (b) PLGA-0.1%G, (c) PLGA-0.5%G and (d) PLGA-1% G samples.

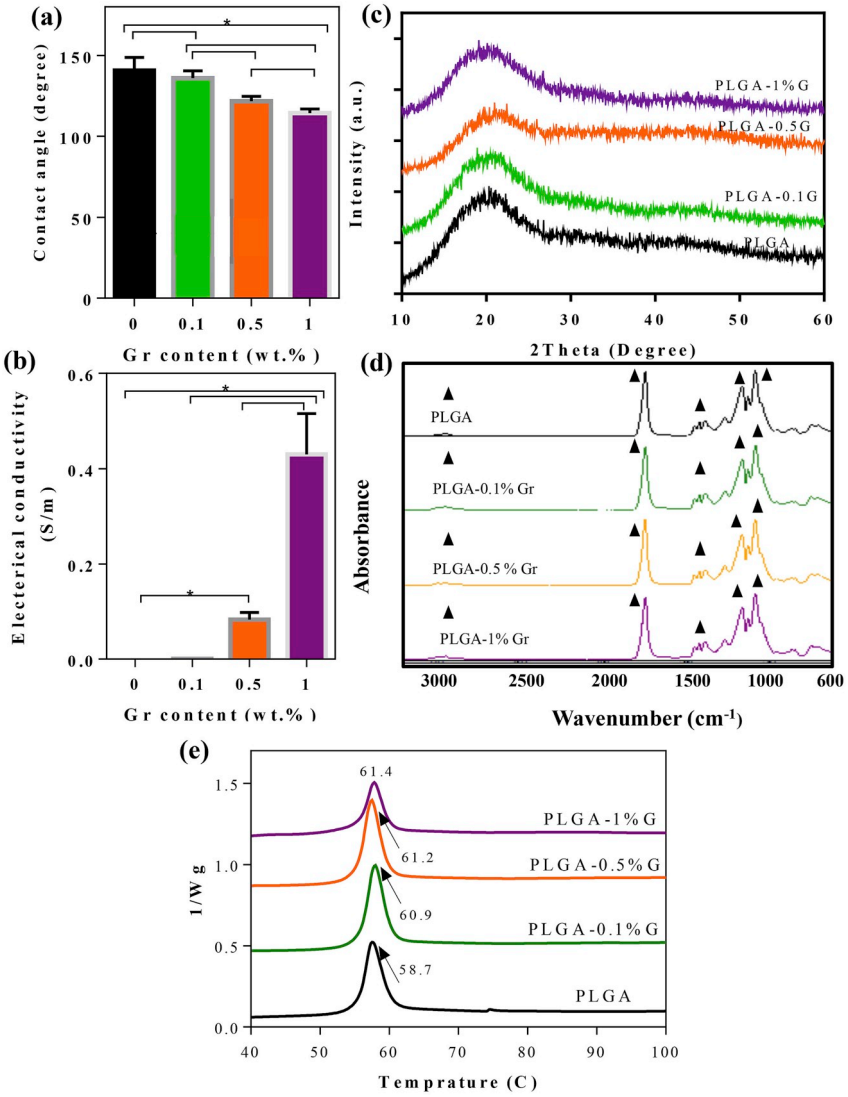

Fig. 3. Chemical properties of aligned PLGA-Gr microribbons: (a) Water contact angle, (b) electrical conductivity (*:P < 0.05), XRD patterns, (b) ATR-FTIR spectra and (d) DSC curves of PLGA and PLGA-Gr microribbons. The T_g of the samples is illustrated on the DSC curves.

demonstrated that the presence of Gr nanosheets in the PLGA microribbons not only could modulate surface topography, but also could control the wettability of surface. According to previous researches, the enhancement in the hydrophilicity of the PLGA-Gr samples could promote the cellular functions such as attachment, proliferation and differentiation, as similarly reported in previous researches [43].

In addition, the conductivity of the PLGA-Gr samples consisting of various amounts of Gr nanosheets was measured using four-point probe method(Fig. 3(b)). Our results demonstrated that the incorporation of Gr nanosheets could significantly promote the electrical conductivity of the PLGA. Noticeably, while PLGA scaffold was an insulator with conductivity of about 0.15 ± 0.01 μS/m, incorporation of 1 wt% Gr nanosheets significantly promoted (for about 10^6 orders) the electrical conductivity to about 0.42 ± 0.03 S/m. The improved electrical conductivity of PLGA via incorporation of Gr nanosheets was similarly reported in previous researches [44]. The promoted electrical conductivity may affect the active synapse formation and consequently may promote the regeneration of nerve tissue.

The chemical composition of the PLGA-Gr microribbons at different concentrations of Gr nanosheets was also studied by XRD analysis (Fig. 3 (c)). Accordingly, the characteristic peak of Gr nanosheets detected at $2\theta = 21.3^\circ$ was overlapped by the broad characteristic peak of PLGA, indicating that most Gr nanosheets were exfoliated and uniformly dispersed in the polymer matrix [45,46]. Furthermore, intensity of the wide peak of PLGA at $2\theta = 21^\circ$ enhanced with increasing the concentration of Gr nanosheets. The same attitude was detected by Meng et al. [47] during the fabrication of electrospun PCL-multiwall carbon nanotube (MWCNT) fibers. This observation could be due to retarding of the flexibility of polymer chains and consequently crystallization improvement of PLGA during the spinning process of PLGA-Gr microribbons [47]. ATR-FTIR spectra of the PLGA-Gr microribbons was also studied to investigate the interaction between Gr and PLGA matrix. According to Fig. 3(d), the spectrum of the PLGA consisted of five characteristic absorbance bands at 2995, 1745, 1452, 1178 and 1091 cm^{-1} which were related to (C–H), (C═O), (O–H), (C–O epoxy) and (C–O alkoxy), respectively (indicated by signs in the spectra) [45]. These peaks could be clearly detected at the spectra of PLGA-graphene microribbons. However, the spectra of PLGA-Gr samples did not show any characteristic peak of Gr nanosheets, due to physical interaction of PLGA and Gr. Soltani et al. [44] similarly evaluated the effect of Gr on the chemical properties of chitosan and PLGA and purposed that FTIR spectra of these polymers did not change during physical interaction with Gr nanosheets. It could be concluded that due to the absence of significant functional groups on the surface of Gr nanosheets, the physical interaction was

occurred between the PLGA matrix and Gr nanosheets and consequently FTIR characteristic peaks of PLGA did not significantly modulate after incorporation of Gr nanosheets, as similarly reported previously [37].

DSC analysis was studied to evaluate the thermal stability of PLGA and PLGA-Gr microribbons (Fig. 3(e)). From DSC curves, the glass transition temperature (T_g) was found to be around 50 °C for PLGA which slightly enhanced with increasing Gr content from 0.1% to 1% in PLGA-Gr microribbons. This increment was due to good dispersion of Gr nanosheets in polymer matrix which could restrict the movement of polymer chains and thus enhancing the crystallinity [45]. Yoon et al. [48] also reported the effect of GO incorporation to PLGA fibers on thermal properties. They investigated that incorporation of GO increased the T_g of composite fibers due to decreased mobility of PLGA chains. They also declared that H-bonding between GO and polymer chains was another reason for reinforcing effect of GO nanosheets on PLGA fibers. In another research, increasing the Tg of PLA-Gr samples with increasing Gr nanosheets was reported confirming our investigations [49].

The mechanical properties of the PLGA and PLGA-Gr microribbons were also evaluated using tensile testing. The representative tensile stress-strain curves of microribbons and data for elastic modulus (E), toughness and tensile strengths are shown in Fig. 4. According to Fig. 4 (a), the tensile properties of PLGA-Gr microribbons increased compared to bared PLGA microribbons. Moreover, according to Fig. 4(b and c), the tensile strength and elastic modulus of PLGA-Gr microribbons were significantly enhanced with increasing Gr nanosheet content ($P < 0.05$). Noticeably, tensile strength and elastic modulus of PLGA microribbons (0.18 ± 0.04 MPa and 5.04 ± 0.5 MPa, respectively) significantly enhanced to 0.4 ± 0.1 MPa and 17.1 ± 1.2 MPa at PLGA-1%G, respectively. This behavior could be attributed to the interfacial interactions between the polymer and Gr nanosheets which could restrict the movement of PLGA chains. Moreover, well-dispersion of Gr nanosheets in a polymer matrix could provide an efficient means for stress transfer and reinforcement in PLGA-Gr microribbons [48,50]. Generally, the mechanical properties are in the increasing mode with enhancement of the Gr content, in the consequence of uniform dispersion of Gr in polymer and good interactions between Gr and polymer matrix during the stirring, ultrasonication and spinning processes [51]. He et al. [37] similarly studied the effect of Gr nanofillers on the enhancement of mechanical properties of alginate-Gr composite fibers. They demonstrated that the tensile strength of alginate fibers enhanced with increasing Gr nanosheets up to 4% in fibers. They could also show the enhancement of Young modulus to the highest amount with 4% loading of G to the polymeric fibers. However, the stress-strain curves revealed that the addition of Gr nanosheets in PLGA matrix led to decrease in elongation as composites became more brittle. The changes of toughness of various samples consisting of various amounts of Gr nanosheets (Fig. 4(d)), confirmed that incorporation of Gr nanosheets significantly reduced the ductility of samples. This behavior was similarly reported for other nanocomposite structures consisting of various kinds of carbon based materials such as carbon nanotube [52,53] and Geraphen [54,55]. The diminishing toughness was initiated most likely by the stiffening role of these nanofillers and improved crystallinity of PLGA.

3.2. Cell culture

The SEM images of the cells cultured on the microribbons are presented in Fig. 5. Clearly, attachment and spreading of the cells enhanced with increasing the concentration of Gr nanosheets. The cells cultured on the PLGA and PLGA-0.1%G microribbons were in the round shapes and could not spread out their filopodia in favor of better attachment. These features improved with increasing the Gr nanosheet concentration from 0.1 to 1 wt%. According to Fig. 5 (c, d), the nano-sized cellular projections by engaging filopodia could be detected at PLGA-Gr samples, showing the cytoskeletal re-organization in favor of cell attachment to underlying substrate and maintaining physical connection with neighboring cells which is essential to support functional cellular regenerations [56]. Lee et al. [57] previously confirmed the superior effect of Gr nanosheets incorporated in the PDMS on the human mesenchymal stem attachment. The cells cultured on PDMS were morphologically

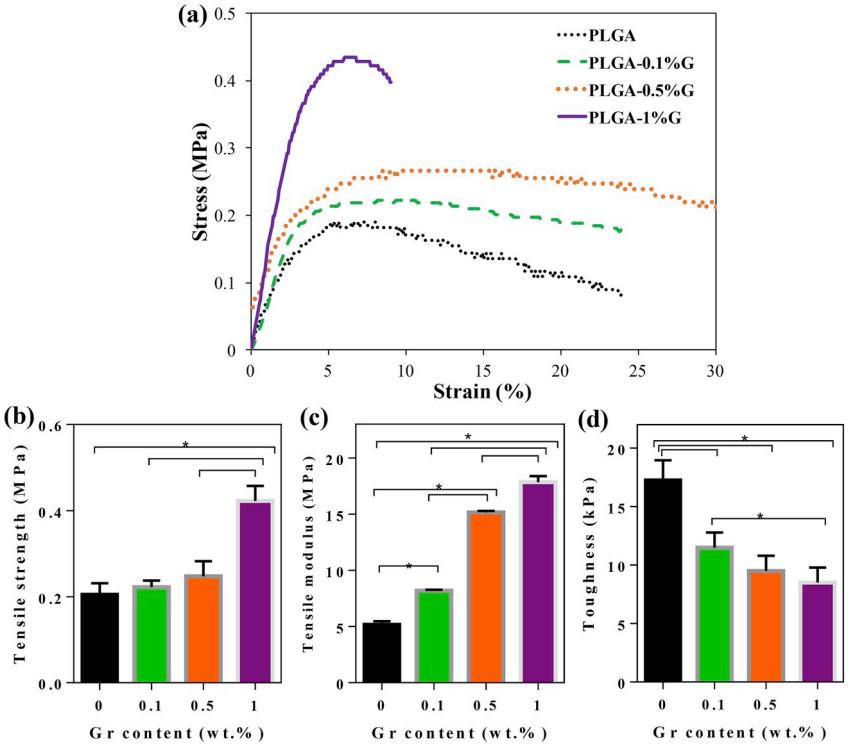

Fig. 4. Mechanical properties of aligned PLGA-Gr microribbons: (a) Tensile stress-strain curves as well as (b) tensile strength, (c) modulus and (d) toughness of PLGA and PLGA-Gr microribbons. (*: $P < 0.05$).

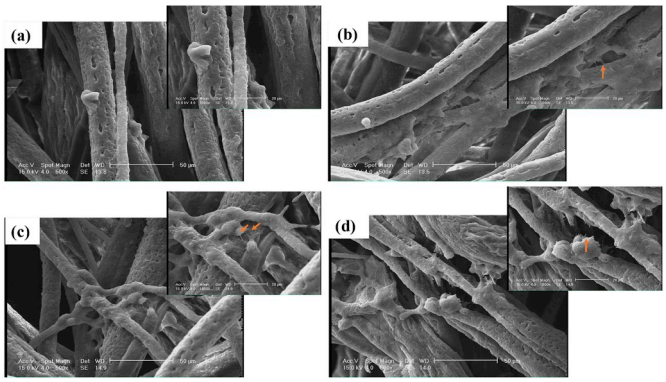

Fig. 5. Biological properties of aligned PLGA-Gr microribbons: SEM images showing the attachment of neuroblasts and neurites extension on (a) PLGA, (b) PLGA-0.1%G, (c) PLGA-0.5%G and (d) PLGA-1%G microribbons.

different from Gr + PDMS substrate. Cells on PDMS tended to acquire spherical shape while the addition of Gr nanosheets contributed to homogenously cell dispersion and filopodial extensions. They showed that more Gr nanosheets deposition on the surface enhanced protein adsorption by π-electron cloud from G side and hydrophobic core of proteins, leading to promoted cell attachment and proliferation rate. We noted extensive neurite-like outgrowth on PLGA-0.5%G and PLGA-1%G samples, supporting the generation of neurite network [22].

The cell viability was also assessed using MTT assay (Fig. 6(a)). Obviously, the PLGA and PLGA-Gr microribbons did not show any cytotoxicity for the cells during 7 days of culture. Based on the data, cell survival increased and reached the highest amount at day 7. Moreover, it seems that the increasing level of Gr nanosheets resulted in a decreased cell survival. In addition, further analysis by flow cytometry technique indicated the positive effect of Gr nanosheets on the proliferation rate of SH-SY5Y cells (Fig. 6(b)). The values reached 33.6% in cells from bared PLGA to 72%, 71.6% and 76.2% after incubation with PLGA-0.1%G, PLGA-0.5%G and PLGA-1%G, respectively. MTT and the flow cytometry assays are two different techniques to measure the proliferation of cells via two different approaches. In addition, the sensitivity of both MTT and flow cytometry assays are different. While MTT assay is based on the evaluation of mitochondrial bioactivity of the target cells on the goal substrates, the flow cytometry analysis could estimate the proliferation potential of cells by monitoring the nuclear factor Ki67, located in distinct sites inside the cells. Based on our data, we could conclude that the scaffold consisting of higher concentration of Gr may have detrimental effects on mitochondrial activity. However, we found a non-significant difference in the proliferation rate of cells exposed to different concentrations of Gr, based on flow cytometry analysis.

Immunofluorescence imaging of SH-SY5Y cells cultured on microribbons stained with MAP-2 (a mature neuron biomarker) is illustrated in Fig. 7. Based on the data, while no cell differentiation was detected for the cells cultured on the PLGA group, increasing amount of Gr nanosheet content from 0.1 wt% to 1 wt% promoted cell maturation and differentiation via the induction of MAP-2 protein. These findings possibly highlighted the positive effect of Gr nanosheets on the cell orientation toward mature neuron type. Moreover, it was discovered that the Gr-based nanomaterials have the ability to enhance the protein synthesis and adhesion in neurons by providing wrinkled and rippled surfaces [58]. In addition, these nanoscale materials could accelerate the regeneration process with their high conductivity rate required for neuronal electrophysiology [58]. Based on the current experiment, we showed that Gr nanosheets incorporated in the PLGA-Gr microribbons played a pivotal role in enhancing the maturation of human neuroblasts. It seems that the enrichment of PLGA backbone with Gr nanosheets could promote a novel cell phenotype via cell adaptation to surface roughness [59].

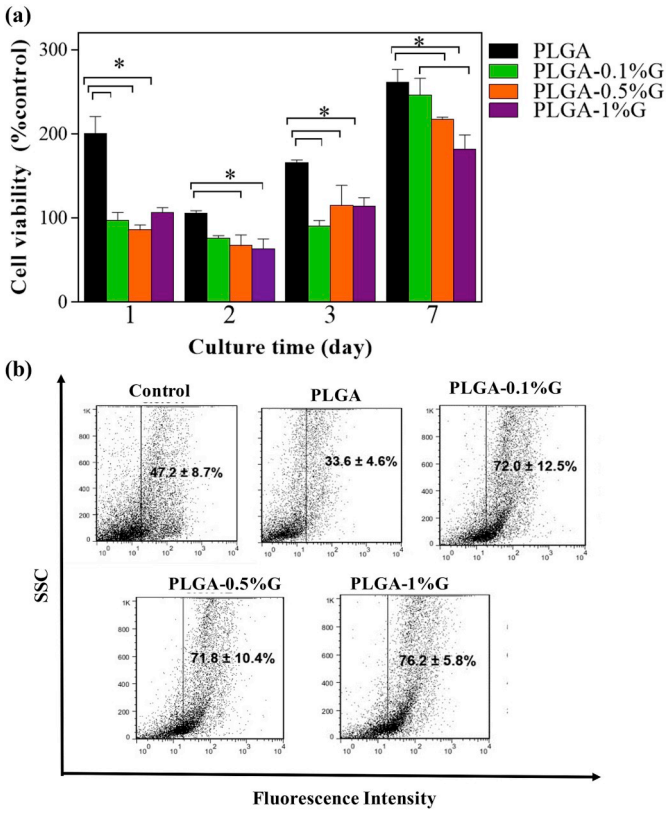

Fig. 6. Biological properties of aligned PLGA-Gr microribbons: (a) cell viability on PLGA and PLGA-Gr microribbons determined using MTT assay (*:P < 0.05). (b)The proliferation of neuroblasts on different microribbons based on Flow cytometry.

Generally, the physical and chemical characteristics of the scaffold are effective to control the cell function [60,61]. In the present study, incorporation of Gr nanosheets could simultaneously control electrical conductivity, mechanical property, hydrophilicity and surface topography of PLGA microribbons leading to modulation of cell functions. In this regard, the size of surface roughness is crucial on the cell adhesion to the distinct surfaces. Nano-size roughness could cluster cell surface integrins, determining cell adhesion capacity and morphology while in the case of micro-size roughness, cell arrangement and maturation by applying focal adhesion mechanisms are more important [62]. Chou et al. [63] proved that small micrometric scale features (25–50 μm) which were close to the dimensions of the cells could be helpful in guiding adhesion and spreading at the single cell scale. It has been established that the cells could be aligned along the groove-like features and changed their shape in the direction of specific grooves [64]. However, the researchers suggested that neural differentiation could take place at both nanoscale and microscale-size features [65]. In this research, formation of aligned microgrooves on the nanocomposite microribbons consisting of high amounts of Gr content along with improvement of hydrophilicity and electrical conductivity of the substrate could promote the adhesion, spreading and differentiation of neural stem cells. In contrary, the expanding of filopodia and favored attachment were not detected in the case of pure PLGA and PLGA-0.1%G microribbons (Fig. 5(a) and b) due to the absence of surface microgrooves, less hydrophilicity and weak electrical conductivity. Similarly, Dowell-Mesfin et al. [66] illustrated that rat hippocampal neurons could grow and extend their neurites on the topography of periodic micropillar after loading on a silicon substrate with 1 μm height. As a result, the axonal reaction was indicated in response to topographies within microscale size pattern. Another important property which could affect cell behavior, is the fiber/microgroove diameter. Bashur et al. [67]

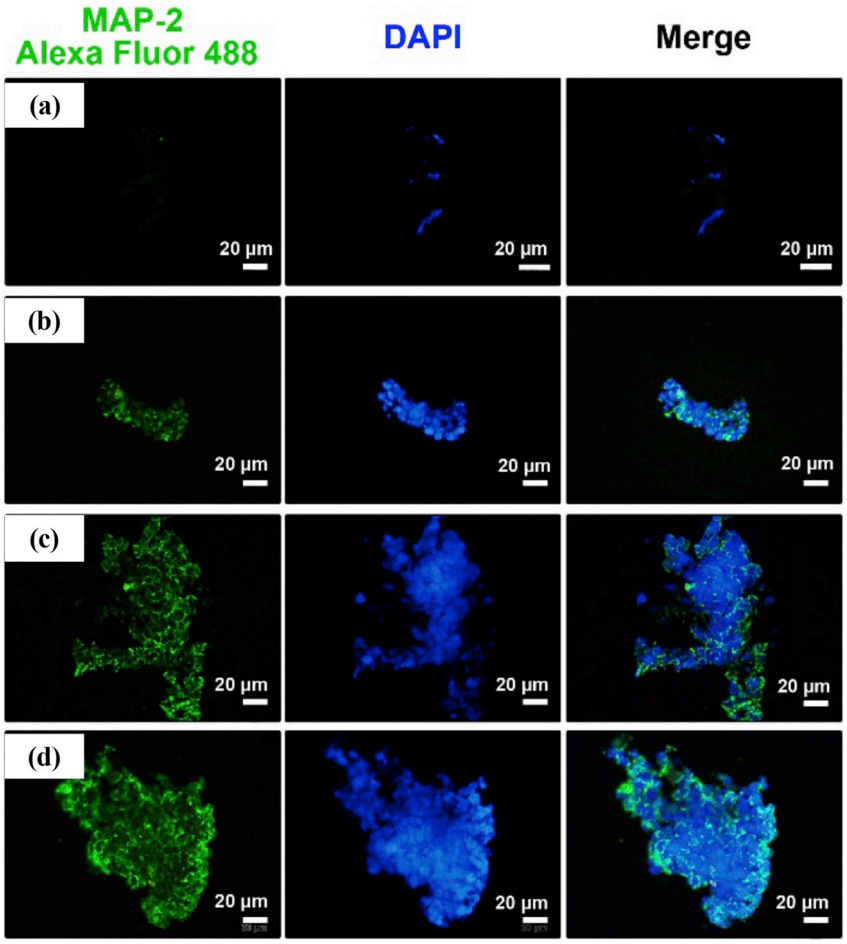

Fig. 7. Biological properties of aligned PLGA-Gr microribbons: Immunofluorescence images of neuroblasts differentiation to mature neurons on (a) PLGA, (b) PLGA-0.1%G, (c) PLGA-0.5%G and (d)PLGA-1%G microribbons.

showed that the fiber diameter of electrospun PLGA was crucial to control the morphology and orientation of fibroblasts. They found that, the critical size of 1 μm was effective in cell alignment and elongation on various types of topographical substrates and could be attributed to the extension of focal adhesion. In this research, we found that incorporation of Gr nanosheets to the polymeric solution resulted in the formation of aligned microgrooves with the size of less than 2 μm on the surface of microribbons. According to Fig. 5(a and b) and Fig. 7, the aligned microribbons without any microgroove on the surface did not have potential to guide the cell attachment and differentiation to mature neurons. In other words, the effect of smaller aligned microgrooves on guiding stem cells for attachment, spreading out the filopodia and differentiation is more than the effect of aligned polymeric ribbons.

4. Conclusion

In summary, highly aligned PLGA-Gr microribbons consisting of various amounts of Gr nanosheets were successfully developed using wet-spinning approach. Encapsulated graphene (Gr) nanosheets improved mechanical properties of the PLGA-Gr constructs, depending on the Gr content. In addition, electrical conductivity and hydrophilicity of PLGA microribbons noticeably promoted with increasing Gr content upon 1 wt%. We also demonstrated the combined effect of Gr nanosheets and aligned microribbons of PLGA with specific aligned nano-feature on the dynamics of neuronal lineage. Moreover, PLGA-Gr microribbons promoted SH-SY5Y cells growth and regulated cell orientation toward mature type phenotype while extending neurite growth. Our results demonstrated that, PLGA-Gr microribbons may have the great potential of applications in the regeneration of central nervous systems.

Acknowledgements

The author should have thanked from Iran National Foundation (INSF, Grant no. 94014204) and Isfahan University of Technology for financial support of this project.

Appendix A. Supplementary data

Supplementary data to this article can be found online at https://doi.org/10.1016/j.compositesb.2019.05.074.

References

[1] Vishwakarma SK, Bardia A, Tiwari SK, Paspala SA, Khan AA. Current concept in neural regeneration research: NSCs isolation, characterization and transplantation in various neurodegenerative diseases and stroke: A review. J Adv Res 2014;5(3):277–94.
[2] Yang S, Leong K-F, Du Z, Chua C-K. The design of scaffolds for use in tissue engineering. Part I. Traditional factors. Tissue Eng 2001;7(6):679–89.
[3] Bini T, Gao S, Wang S, Ramakrishna S. Poly (l-lactide-co-glycolide) biodegradable microfibers and electrospun nanofibers for nerve tissue engineering: an in vitro study. J Mater Sci 2006;41(19):6453–9.
[4] Roach P, Parker T, Gadegaard N, Alexander MR. A bio-inspired neural environment to control neurons comprising radial glia, substrate chemistry and topography. Biomater Sci 2013;1(1):83–93.
[5] Pan Z, Ding J. Poly (lactide-co-glycolide) porous scaffolds for tissue engineering and regenerative medicine. Interface Focus 2012;2(3):366–77.
[6] Bible E, Chau DY, Alexander MR, Price J, Shakesheff KM, Modo M. The support of neural stem cells transplanted into stroke-induced brain cavities by PLGA particles. Biomaterials 2009;30(16):2985–94.

[7] Lee JY, Bashur CA, Goldstein AS, Schmidt CE. Polypyrrole-coated electrospun PLGA nanofibers for neural tissue applications. Biomaterials 2009;30(26):4325–35.
[8] Golafshan N, Kharaziha M, Fathi M. Tough and conductive hybrid graphene-PVA: Alginate fibrous scaffolds for engineering neural construct. Carbon 2017;111: 752–63.
[9] Yang J, Shi G, Bei J, Wang S, Cao Y, Shang Q, Yang G, Wang W. Fabrication and surface modification of macroporous poly (lactic acid) and poly (L-lactic-co-glycolic acid)(70/30) cell scaffolds for human skin fibroblast cell culture. Biomed Mater Res B 2002;62(3):438–46.
[10] Hatten ME. Riding the glial monorail: a common mechanism for glialguided neuronal migration in different regions of the developing mammalian brain. Trends Neurosci 1990;13(5):179–84.
[11] Mammadov B, Sever M, Guler MO, Tekinay AB. Neural differentiation on synthetic scaffold materials. Biomater Sci 2013;1(11):1119–37.
[12] Miller C, Jeftinija S, Mallapragada S. Synergistic effects of physical and chemical guidance cues on neurite alignment and outgrowth on biodegradable polymer substrates 2002;8(3):367–78.
[13] Miller C, Shanks H, Witt A, Rutkowski G, Mallapragada S. Oriented Schwann cell growth on micropatterned biodegradable polymer substrates. Biomaterials 2001; 22(11):1263–9.
[14] Rajnicek A, Britland S, McCaig C. Contact guidance of CNS neurites on grooved quartz: influence of groove dimensions, neuronal age and cell type. J Cell Sci 1997; 110(23):2905–13.
[15] Clark P, Connolly P, Curtis A, Dow J, Wilkinson CD. Topographical control of cell behaviour: II. Multiple grooved substrata. Development 1990;108(4):635–44.
[16] Mahoney MJ, Chen RR, Tan J, Saltzman WM. The influence of microchannels on neurite growth and architecture. Biomaterials 2005;26(7):771–8.
[17] Foley JD, Grunwald EW, Nealey PF, Murphy CJ. Cooperative modulation of neuritogenesis by PC12 cells by topography and nerve growth factor. Biomaterials 2005;26(17):3639–44.
[18] Lee MR, Kwon KW, Jung H, Kim HN, Suh KY, Kim K, Kim K-S. Direct differentiation of human embryonic stem cells into selective neurons on nanoscale ridge/groove pattern arrays. Biomaterials 2010;31(15):4360–6.
[19] Mattotti M, Alvarez Z, Ortega JA, Planell JA, Engel E, Alcántara S. Inducing functional radial glia-like progenitors from cortical astrocyte cultures using micropatterned PMMA. Biomaterials 2012;33(6):1759–70.
[20] Callahan LAS, Xie S, Barker IA, Zheng J, Reneker DH, Dove AP, Becker ML. Directed differentiation and neurite extension of mouse embryonic stem cell on aligned poly (lactide) nanofibers functionalized with YIGSR peptide. Biomaterials 2013;34(36):9089–95.
[21] Corey JM, Lin DY, Mycek KB, Chen Q, Samuel S, Feldman EL, Martin DC. Aligned electrospun nanofibers specify the direction of dorsal root ganglia neurite growth. J Biomed Mater Res Part A: An Official Journal of The Society for Biomaterials, The Japanese Society for Biomaterials, and The Australian Society for Biomaterials and the Korean Society for Biomaterials 2007;83(3):636–45.
[22] Yang F, Murugan R, Wang S, Ramakrishna S. Electrospinning of nano/micro scale poly (L-lactic acid) aligned fibers and their potential in neural tissue engineering. Biomaterials 2005;26(15):2603–10.
[23] Hurtado A, Cregg JM, Wang HB, Wendell DF, Oudega M, Gilbert RJ, McDonald JW. Robust CNS regeneration after complete spinal cord transection using aligned poly-L-lactic acid microfibers. Biomaterials 2011;32(26):6068–79.
[24] Shimizu T, Yamato M, Kikuchi A, Okano T. Cell sheet engineering for myocardial tissue reconstruction. Biomaterials 2003;24(13):2309–16.
[25] Harrington H, Cato P, Salazar F, Wilkinson M, Knox A, Haycock JW, Rose F, Aylott JW, Ghaemmaghami AM. Immunocompetent 3D model of human upper airway for disease modeling and in vitro drug evaluation. Mol Pharm 2014;11(7): 2082–91.
[26] Nelson KD, Romero A, Waggoner P, Crow B, Borneman A, Smith GM. Technique paper for wet-spinning poly (L-lactic acid) and poly (DL-lactide-co-glycolide) monofilament fibers. Tissue Eng 2003;9(6):1323–30.
[27] Koh H, Yong T, Chan C, Ramakrishna S. Enhancement of neurite outgrowth using nano-structured scaffolds coupled with laminin. Biomaterials 2008;29(26): 3574–82.
[28] Kuo Y-C, Yeh C-F. Effect of surface-modified collagen on the adhesion, biocompatibility and differentiation of bone marrow stromal cells in poly (lactide-co-glycolide)/chitosan scaffolds. Colloids Surfaces B Biointerfaces 2011;82(2): 624–31.
[29] Lee JY, Bashur CA, Goldstein AS, Schmidt CE. Polypyrrole-coated electrospun PLGA nanofibers for neural tissue applications. Biomaterials 2009;30(26): 4325–35.
[30] Shuai C, Li Y, Wang G, Yang W, Peng S, Feng P. Surface modification of nanodiamond: toward the dispersion of reinforced phase in poly-l-lactic acid scaffolds. Int J Biol Macromol 2019;126:1116–24.
[31] Li N, Zhang X, Song Q, Su R, Zhang Q, Kong T, Liu L, Jin G, Tang M, Cheng G. The promotion of neurite sprouting and outgrowth of mouse hippocampal cells in culture by graphene substrates. Biomaterials 2011;32(35):9374–82.
[32] Shuai C, Feng P, Gao C, Shuai X, Xiao T, Peng S. Graphene oxide reinforced poly (vinyl alcohol): nanocomposite scaffolds for tissue engineering applications. RSC Adv 2015;5(32):25416–23.
[33] Bitounis D, Ali-Boucetta H, Hong BH, Min DH, Kostarelos K. Prospects and challenges of graphene in biomedical applications. Adv Mater 2013;25(16): 2258–68.
[34] Akhavan O, Ghaderi E, Abouei E, Hatamie S, Ghasemi E. Accelerated differentiation of neural stem cells into neurons on ginseng-reduced graphene oxide sheets. Carbon 2014;66:395–406.
[35] Shah S, Yin PT, Uehara TM, Chueng STD, Yang L, Lee KB. Guiding stem cell differentiation into oligodendrocytes using graphene-nanofiber hybrid scaffolds. Adv Mater 2014;26(22):3673–80.
[36] Kabiri M, Oraee-Yazdani S, Shafiee A, Hanaee-Ahvaz H, Dodel M, Vaseei M, Soleimani M. Neuroregenerative effects of olfactory ensheathing cells transplanted in a multi-layered conductive nanofibrous conduit in peripheral nerve repair in rats. J Biomed Sci 2015;22(1):35.
[37] He Y, Zhang N, Gong Q, Qiu H, Wang W, Liu Y, Gao J. Alginate/graphene oxide fibers with enhanced mechanical strength prepared by wet spinning. Carbohydr Polym 2012;88(3):1100–8.
[38] Johansson F, Carlberg P, Danielsen N, Montelius L, Kanje M. Axonal outgrowth on nano-imprinted patterns. Biomaterials 2006;27(8):1251–8.
[39] Um IC, Kweon H, Lee KG, Ihm DW, Lee J-H, Park YH. Wet spinning of silk polymer: I. Effect of coagulation conditions on the morphological feature of filament. Int J Biol Macromol 2004;34(1–2):89–105.
[40] Zhang J, Wang L, Zhu M, Wang L, Xiao N, Kong D. Wet-spun poly (ε-caprolactone) microfiber scaffolds for oriented growth and infiltration of smooth muscle cells. Mater Lett 2014;132:59–62.
[41] Pinto AM, Moreira S, Gonçalves IC, Gama FM, Mendes AM, Magalhães FD. Biocompatibility of poly (lactic acid) with incorporated graphene-based materials. Colloids Surfaces B Biointerfaces 2013;104:229–38.
[42] Knauert ST, Douglas JF, Starr FW. The effect of nanoparticle shape on polymer-nanocomposite rheology and tensile strength. J Polym Sci B Polym Phys 2007;45 (14):1882–97.
[43] Fu C, Bai H, Hu Q, Gao T, Bai Y. Enhanced proliferation and osteogenic differentiation of MC3T3-E1 pre-osteoblasts on graphene oxide-impregnated PLGA–gelatin nanocomposite fibrous membranes. RSC Adv 2017;7(15):8886–97.
[44] Soltani S, Ebrahimian-Hosseinabadi M, Kharazi AZ. Chitosan/graphene and poly (D, L-lactic-co-glycolic acid)/graphene nano-composites for nerve tissue engineering. Tissue Eng Regen Med 2016;13(6):684–90.
[45] Yoon OJ, Jung CY, Sohn IY, Kim HJ, Hong B, Jhon MS, Lee N-E. Nanocomposite nanofibers of poly (D, L-lactic-co-glycolic acid) and graphene oxide nanosheets. Compos Appl Sci Manuf 2011;42(12):1978–84.
[46] Shin YC, Lee JH, Jin L, Kim MJ, Kim Y-J, Hyun JK, Jung T-G, Hong SW, Han D-W. Stimulated myoblast differentiation on graphene oxide-impregnated PLGA-collagen hybrid fibre matrices. J Nanobiotechnol 2015;13(1):21.
[47] Meng Z, Zheng W, Li L, Zheng Y. Fabrication and characterization of three-dimensional nanofiber membrance of PCL–MWCNTs by electrospinning. Mater Sci Eng C 2010;30(7):1014–21.
[48] Yoon OJ, Sohn IY, Kim DJ, Lee N-E. Enhancement of thermomechanical properties of poly (D, L-lactic-co-glycolic acid) and graphene oxide composite films for scaffolds. Macromol Res 2012;20(8):789–94.
[49] Chen Y, Yao X, Zhou X, Pan Z, Gu Q. Poly (lactic acid)/graphene nanocomposites prepared via solution blending using chloroform as a mutual solvent. J Nanosci Nanotechnol 2011;11(9):7813–9.
[50] Ji X, Xu Y, Zhang W, Cui L, Liu J. Review of functionalization, structure and properties of graphene/polymer composite fibers. Compos Appl Sci Manuf 2016; 87:29–45.
[51] Wan C, Chen B. Poly (ε-caprolactone)/graphene oxide biocomposites: mechanical properties and bioactivity. Biomed Mater 2011;6(5):055010.
[52] Liu Y, Lu J, Xu G, Wei J, Zhang Z, Li X. Tuning the conductivity and inner structure of electrospun fibers to promote cardiomyocyte elongation and synchronous beating. Mater Sci Eng C 2016;69:865–74.
[53] Kumar S, Bose S, Chatterjee K. Amine-functionalized multiwall carbon nanotubes impart osteoinductive and bactericidal properties in poly (ε-caprolactone) composites. RSC Adv 2014;4(3):19086–98.
[54] Esrafilzadeh D, Jalili R, Stewart E, Aboutalebi S, Razal J, Moulton S, Wallace G. High-performance multifunctional graphene-PLGA fibers: toward biomimetic and conducting 3D scaffolds. Adv Funct Mater 2016;26(18):3105–17.
[55] Wan C, Chen B. Reinforcement and interphase of polymer/graphene oxide nanocomposites. J Mater Chem 2012;22(8):3637–46.
[56] Wang HB, Mullins ME, Cregg JM, McCarthy CW, Gilbert RJ. Varying the diameter of aligned electrospun fibers alters neurite outgrowth and Schwann cell migration. Acta Biomater 2010;6(8):2970–8.
[57] Lee WC, Lim CHY, Shi H, Tang LA, Wang Y, Lim CT, Loh KP. Origin of enhanced stem cell growth and differentiation on graphene and graphene oxide. ACS Nano 2011;5(9):7334–41.
[58] Ryu S, Kim B-S. Culture of neural cells and stem cells on graphene. Tissue Eng Regen Med 2013;10(2):39–46.
[59] Kim T-H, Shah S, Yang L, Yin PT, Hossain MK, Conley B, Choi J-W, Lee K-B. Controlling differentiation of adipose-derived stem cells using combinatorial graphene hybrid-pattern arrays. ACS Nano 2015;9(4):3780–90.
[60] Correa-Duarte MA, Wagner N, Rojas-Chapana J, Morsczeck C, Thie M, Giersig M. Fabrication and biocompatibility of carbon nanotube-based 3D networks as scaffolds for cell seeding and growth. Nano Lett 2004;4(11):2233–6.
[61] Qi Y, Tai Z, Sun D, Chen J, Ma H, Yan X, Liu B, Xue Q. Fabrication and characterization of poly (vinyl alcohol)/graphene oxide nanofibrous biocomposite scaffolds. J Appl Polym Sci 2013;127(3):1885–94.
[62] Nguyen AT, Sathe SR, Yim EK. From nano to micro: topographical scale and its impact on cell adhesion, morphology and contact guidance. J Phys Condens Matter 2016;28(18):183001.
[63] Chou C-L, Rivera AL, Sakai T, Caplan AI, Goldberg VM, Welter JF, Baskaran H. Micrometer scale guidance of mesenchymal stem cells to form structurally oriented cartilage extracellular matrix. Tissue Eng 2012;19(9–10):1081–90.

[64] Wilkinson C, Riehle M, Wood M, Gallagher J, Curtis A. The use of materials patterned on a nano-and micro-metric scale in cellular engineering. Mater Sci Eng C 2002;19(1–2):263–9.
[65] López-Fagundo C, Mitchel JA, Ramchal TD, Dingle Y-TL, Hoffman-Kim D. Navigating neurites utilize cellular topography of Schwann cell somas and processes for optimal guidance. Acta Biomater 2013;9(7):7158–68.
[66] Dowell-Mesfin N, Abdul-Karim M, Turner A, Schanz S, Craighead H, Roysam B, Turner J, Shain W. Topographically modified surfaces affect orientation and growth of hippocampal neurons. J Neural Eng 2004;1(2):78.
[67] Bashur CA, Dahlgren LA, Goldstein AS. Effect of fiber diameter and orientation on fibroblast morphology and proliferation on electrospun poly (D, L-lactic-co-glycolic acid) meshes. Biomaterials 2006;27(33):5681–8.